

Accepted by PASP, 5 September 2012

The Stony Brook / SMARTS Atlas of (mostly) Southern Novae

Frederick M. Walter, Andrew Battisti¹ & Sarah E. Towers²

Department of Physics and Astronomy, Stony Brook University, Stony Brook, NY 11794-3800

Howard E. Bond

Space Telescope Science Institute, Baltimore MD 21218³

Guy S. Stringfellow

Center for Astrophysics and Space Astronomy, University of Colorado, Boulder CO 80309

ABSTRACT

We introduce the Stony Brook / SMARTS Atlas of (mostly) Southern Novae. This atlas contains both spectra and photometry obtained since 2003. The data archived in this atlas will facilitate systematic studies of the nova phenomenon and correlative studies with other comprehensive data sets. It will also enable detailed investigations of individual objects. In making the data public we hope to engender more interest on the part of the community in the physics of novae. The atlas is on-line at <http://www.astro.sunysb.edu/fwalter/SMARTS/NovaAtlas/>.

Subject headings: novae, cataclysmic variables, accretion disks

1. Introduction

Exploding stars have been noted for millennia, and observed (in a scientific sense) for somewhat over a century. It wasn't until the middle of the 20th century that a distinction could be made between the supernovae, the novae, and the eruptive phenomena seen in cataclysmic variables (the dwarf novae). Kraft (1963) was the first to suggest that the novae were the consequence of explosive hydrogen burning on the surface of a degenerate dwarf. It is now well accepted that the novae are manifestations of runaway thermonuclear reactions on the surface of a white dwarf (WD) accreting

¹now at Dept of Astronomy, University of Massachusetts, Amherst MA 01003

²now at Dept of Physics, Western Michigan University, Kalamazoo MI, 49008

³current address: 9615 Labrador Ln., Cockeysville, MD 21030

hydrogen in a close binary system (e.g., Starrfield 1971). The novae are highly dynamic phenomena, with timescales ranging from seconds to millennia, occurring in complex systems involving two stars and mass transfer.

The primary driver of the evolution of the observational characteristics of a nova is the temporal decrease of the optical depth in an expanding atmosphere. The novae are marked by an extraordinary spectral evolution (Williams 1991, 1992). In the initial phases one often sees an optically thick, expanding pseudo-photosphere. In some cases one sees the growth and then disappearance of inverse P Cygni absorption lines from the cool, high velocity ejecta. As the pseudo-photosphere becomes optically thin, emission lines of the Hydrogen Balmer series strengthen, accompanied by either a spectrum dominated by permitted lines of Fe II, or of helium and nitrogen. The emission line profiles and line ratios evolve as the optical depth of the ejecta decreases, and the nova transitions from the permitted to the nebular phase (Williams 1991).

Beyond this template, in detail the novae exhibit a panoply of individual behaviors. Payne-Gaposchkin (1957) and McLaughlin (1960) described the evolution of novae as they were known at the time. Williams (1992) discussed the formation of the lines, and divided novae into the Fe II and He-N classes, based on which emission lines dominated (aside from the ubiquitous Balmer lines of hydrogen). Novae are also categorized as recurrent and classical novae, with the former having more than one recorded outburst. Over a long enough baseline, it is likely that all novae are recurrent (e.g., Ford 1978).

Bode & Evans (2008) present a recent set of reviews of the nova phenomenon.

There exist well-sampled photometric records for many novae, such as those presented by Strobe et al. (2010). They classify the photometric light curves, from plates amassed over the past century, into 7 distinct photometric classes. On the other hand, spectroscopic observations of novae have rarely been pursued far past maximum because most novae fade rapidly, and time on the large telescopes required for spectroscopy is precious. The most comprehensive past work was the Tololo Nova atlas (Williams et al. 1994) of 13 novae followed spectroscopically over a 5 year interval. The availability of the SMARTS¹ telescope facilities (Subasavage et al. 2010) makes possible routine synoptic monitoring programs, both photometric and spectroscopic, of time-variable sources. It is timely, therefore, to undertake a comprehensive, systematic, high-cadence study of the spectrophotometric evolution of the galactic novae.

This atlas collects photometry and spectra of the novae we have observed with SMARTS. Most of the novae in the atlas are recent novae, discovered since 2003. Most are in the southern hemisphere. The observing cadences are irregular; we have concentrated on He-N and recurrent novae, novae in the LMC, and novae that otherwise show unusual characteristics.

¹The Small and Medium Aperture Telescope System, directed by Charles Bailyn, is an ever-evolving partnership that has overseen operations of 4 small telescopes at Cerro Tololo Interamerican Observatory since 2003.

Our purpose here is to introduce this atlas. Our scientific aim is to facilitate a detailed comparison of the various characteristics of the novae. These data can be used by and of themselves to study individual objects, for systematic studies to further define the phenomenon, and for correlative studies with other comprehensive data sets, such as the *Swift* Nova Working Group’s survey of X-ray and UV observations of recent novae (Schwarz et al. 2011). Our aim in making the atlas public is to make the data accessible to the community. We are focusing on certain novae, and on particular aspects of the nova phenomenon (§5), but simply cannot do justice to the full dataset.

2. Observations and Data Analysis

2.1. Low Dispersion Spectroscopy

The spectra reported here have been obtained with the venerable RC spectrograph² on the SMARTS/CTIO 1.5m telescope. Observations are queue-scheduled, and are taken by dedicated service observers.

The detector is a Loral 1K CCD. We use a variety of spectroscopic modes, with most of the spectra having been obtained with one of the standard modes shown in Table 1.

We use slit widths of 1 and 0.8 arcsec in the low and the higher resolution 47/II modes, respectively. The slit is oriented E-W and is not rotated during the night.

We routinely obtain 3 spectra of each target in order to filter for cosmic rays. We combine the 3 images and extract the spectrum by fitting a Gaussian in the spatial direction at each pixel. Wavelength calibration is accomplished by fitting a 3rd to 6th order polynomial to the Th-Ar or Ne calibration lamp line positions. We observe a spectrophotometric standard star, generally LTT 4364 (Hamuy et al. 1992, 1994) or Feige 110 (Oke 1990; Hamuy et al. 1992, 1994), on most nights to determine the counts-to-flux conversion. Because of slit losses, possible changes in transparency and seeing during the night, and parallactic losses due to the fixed slit orientation, the flux calibration is imprecise. We generally recover the correct spectral shape, except at the shortest wavelengths (<3800Å) where apparent changes in the slope of the continuum are likely attributable to airmass-dependent parallactic slit losses. We have the capability to use simultaneous or contemporaneous photometry to recalibrate the spectra.

There are some quality control issues that have not been fully dealt with, especially when we are near the sensitivity limits of the telescope. These include observations of an incorrect star, obviously incorrect flux calibrations, or spectra indistinguishable from noise. We are going through the data as time permits to address these issues.

²<http://www.ctio.noao.edu/spectrographs/60spec/60spec.html>

2.2. High Dispersion Spectroscopy

We have a small number of high resolution spectra of some of the brighter novae near maximum. These were obtained with the Bench-Mounted Echelle³, and currently with the Chiron echelle spectrograph⁴. These data will be incorporated into the atlas at a later time.

2.3. Photometry

Most of the photometry was obtained using the ANDICAM⁵ dual-channel imager on the 1.3m telescope. Observations are queue-scheduled, with dedicated service observers.

The ANDICAM optical channel is a 2048² pixel Fairchild 447 CCD. It is read out with 2x2 binning, which yields a 0.369 arcsec/pixel plate scale. The field of view is roughly 6x6 arcmin, but until recently there has been significant unusable area on the east and south sides on the chip. The finding charts in the atlas show examples of ANDICAM images. We normally obtain single images, since the fraction of pixels marred by cosmic rays and other events is small. Exposure times range from 1 second to about 2 minutes. We use the standard Johnson-Kron-Cousins B , V , R_C , and I_C filters (the U filter has been unavailable since 2005, but we have extensive U band for some of the earlier novae, particularly V475 Sct and V5114 Sgr).

The ANDICAM IR channel is a Rockwell 1024² HgCdTe “Hawaii” Array. It is read out in 4 quadrants with 2x2 binning, which yields a 0.274 arcsec/pixel plate scale and a 2.4 arcmin field of view. The observations are dithered using an internal mirror. In most cases we use 3 dither positions, with integration times from 4 seconds (the minimum integration time) to about 45 seconds. We use the CIT/CTIO J , H , and K_s filter set.

The optical and IR channels are observed simultaneously using a dichroic beam splitter. The observing cadence varies from nightly for new novae to \sim annual monitoring for the oldest novae in our list.

We perform aperture photometry on the target and between 1 and 25 comparison stars in the field. The aperture radius R is either 5 or 7 pixels, depending on field crowding and sky brightness. The background is the median value in an annulus of inner radius $2R$ and outer radius $2R+20$ pixels centered on the extraction aperture. Instrumental magnitudes are recorded for each star. There are cases where the fading remnant becomes blended with nearby stars (within ~ 1.5 arcsec). To date we have not accounted for such blending. Eventually we plan to employ PSF-fitting techniques in these crowded regions.

³<http://www.ctio.noao.edu/noao/content/fiber-echelle-spectrograph>

⁴<http://www.ctio.noao.edu/noao/content/chiron>

⁵<http://www.astronomy.ohio-state.edu/ANDICAM/detectors.html>

On most photometric nights an observation of a Landolt (1992) standard field is taken. On those nights we determine the zero-point correction and determine the magnitudes of the comparison stars. We adopt the mean magnitudes for each comparison star. These are generally reproducible to better than 0.02 mag; variable stars are identified through their scatter around the mean, and are not used in the differential photometry. With only a single observation of a standard star field each night, we assume the nominal atmospheric extinction law and zero color correction. Using differential photometry, we can recover the apparent magnitude of a target with a typical uncertainty of <0.03 mag at 20^{th} magnitude.

While we could do the same with the IR channel images, we find it simpler to use the catalogued 2MASS magnitudes of the standard stars. We implicitly assume that the 2MASS comparison stars are non-variable, and that the color terms in the photometric solution are negligible.

In addition, some higher cadence data have been obtained with the SMARTS 0.9m and 1.0m telescopes. The 0.9m detector is a 2048x2046 CCD with a 0.401 arcsec/pixel plate scale. On the 1.0m, we used the 512x512 Apogee camera that was employed prior to installation of the 4K camera. We perform the differential photometry in a manner identical to that for the ANDICAM, and merge the data sets. These data are not yet fully incorporated into the atlas.

3. Setup of the Atlas

The atlas is on-line at <http://www.astro.sunysb.edu/fwalter/SMARTS/NovaAtlas/>.

The atlas consists of a main page for each nova, giving finding charts (in both V and K bands), coordinates, and links to the spectra and photometry. The spectra are available as images, and may be downloaded in ascii (text) format. The photometry page shows plots of the light curve and colors, and permits one to download the data in ascii format. Note that the plots on the photometry page only show data with formal uncertainties <0.5 mag, while all measured magnitudes and uncertainties are included in the ascii listings. There is a link to a page of references for other observations of the novae.

4. The Novae

As of 1 July 2012 the atlas includes data on 64 novae. Of these, 29 are still bright enough ($V < 18$) to reach spectroscopically with the 1.5m/RC spectrograph. Most are still detectable photometrically with the 1.3m/ANDICAM imager. Only 5 are no longer on our photometric target list because they are too faint or too confused with brighter companions.

The spatial distribution of these novae is shown in Figure 1 in both celestial and galactic coordinates.

Lists of our targets and particulars on the number and observing date distribution of the observations are in Tables 2 (novae from before 2012); 3 (novae discovered in 2012), and 4 (novae in the LMC). The reference time is ideally the time of peak brightness, but this is often not well known. In general, T_0 is the time of discovery. In the case of T Pyx, which rises very slowly, T_o is the time of peak brightness as estimated from our photometry. For novae that were discovered well past peak, including N Sgr 2012b and XMMU J115113.3-623730, T_0 is a guess. All the dates in the Tables are referenced to T_0 . The tabulated V is the last observed V magnitude; in most cases this is the brightness in June 2012. The Tables are current as of 1 July 2012.

4.1. Observing Statistics

As of 1 July 2012 the full atlas contains 64 novae. We have between 1 and 368 spectra for the novae, with a median of 28 spectra per nova. The number of photometric points varies between 1 and 265, with a median of 35, for 53 novae. Since some of the observations were taken through thick clouds, not all observations have the best possible S/N.

The photometric and spectral coverage is generally non-uniform in time. In addition to annual gaps due to the Sun, there is spotty coverage during the austral winter when the weather becomes worse. We do not have unlimited observing time, so we concentrate on those novae that tickle our astronomical fancy - the He-N novae, and those showing unusual characteristics. We do not attempt spectroscopy of targets fainter than $V \sim 18$, because the 1.5m telescope has limited grasp.

We generally do not make great efforts to obtain photometry from day 0, because amateur astronomers do such a good job. In many cases data available from the AAVSO can fill in the first few weeks, while the nova is bright (we do have bright limits near $V = 8$ and $K = 6$). Our forte is the ability to a) follow the evolution to quiescence, and b) to do so in the 7 photometric bands from B through K_s . In one case we were on the nova 1.1 days after discovery, but the median delay is 15 days.

We try to start the spectroscopic monitoring sooner, because this is a unique capability of SMARTS. The first spectrum is obtained with a median delay of 8.0 days from discovery, but we have observed 1 nova within 0.6 days of discovery, 9 within 2 days, and 14 within 3 days.

We have multi-epoch photometry of 52 novae over timespans of up to 3173 days (8.7 years), and multi-epoch spectroscopy of 63 novae over timespans of up to 3156 days (8.6 years). These durations will increase with time so long as SMARTS continues operating, and the targets are sufficiently bright. The median observation durations of 1317 and 360 days, respectively, for the photometry and spectroscopy, are limited mostly by target brightness. The median time between observations is skewed by the growing number of old, faint targets that are now observed with a cadence of 1-2 observations per year, so that the median time between spectra is 8.4 days, and is 27 days for photometric observations.

4.2. The Example of V574 Pup

We illustrate possible uses of the atlas with the example of V574 Pup, an Fe II nova for which we have good coverage. Aside from near-IR observations (Naik et al. 2010) and analysis of the super-soft X-ray source (Schwarz et al. 2011), there has been little discussion of this bright nova.

The main atlas page (Figure 2) presents finding charts in V and K , along with the coordinates, time of discovery, and links to the spectral and photometric data and references.

The photometry consists of observations taken on 100 days with the 1.3m ANDICAM imager, starting on day 32 and running through day 2723 (5 May 2012). Most of these sets include all 7 ANDICAM bands, $BVRIJHK_s$. This light curve is shown in Figure 3. It is possible to fill in the first 30 days with data from other sources, such as Siliverio et al. (2005), or by using data from the AAVSO (www.aavso.org).

We supplemented these with data taken on 20 days using a temporary small CCD on the SMARTS 1.0m telescope. These were opportunistic observations enabled by the unavailability of the wide-field 4k camera. We use the ~ 2 hour long sequences to search for short periodicities. (Similar data exist for very few of the novae in the atlas.) Three long sequences in the B band, on days 87, 195, and 196, showed sinusoidal-like modulations. Removing a linear trend from the data on day 87 and normalizing to the mean magnitudes, we find a likely period of 0.0472 days (68 minutes; see Figure 4) from a shortest-string analysis (Dworetzky 1983). However, we cannot exclude some aliases. This is shorter than the minimum orbital period for CVs, and may be half an orbital period (ellipsoidal variability is a possible explanation). The amplitude of the best-fit sinusoid decreased from 0.02 to 0.007 mag from day 87 to days 195-196.

We obtained 107 spectra before the target became too faint for the 1.5m telescope. We illustrate two types of investigations that can be supported by high cadence spectral observations.

1. Figure 5 shows the evolution of the P Cygni line profiles as the wind evolves against the backdrop of the optically-thick pseudo-photosphere. With daily spectra, it is clear that the absorption velocities are not constant, but rather are accelerating. Through day 14 the velocities can be described as a quadratic function of time. Hence the acceleration is linear in time. It is hard to see how this can result from decreasing optical depth effects in an envelope with a monotonic velocity law increasing outwards. Shore et al. (2011) show how similar structures seen in T Pyx can be explained as an outward-moving recombination front in an envelope with a linear velocity law.
2. Figure 6 shows the time-evolution of a series of lines of differing temperatures as the nova evolves through the nebular and coronal phases. The [Fe X] $\lambda 6375\text{\AA}$ line requires high excitation, and its presence correlates well with the super-soft (SSS) X-ray emitting phase (Schwarz et al. 2011). V574 Pup was in its SSS phase from before day 180 through day 1118; it ended before day 1312. We can use data such as these to explore how well optical lines are

diagnostic of the SSS phase.

4.3. Notes on the Novae

Notes here are not meant to be complete or definitive in any sense. They are meant to highlight past or ongoing work on select novae, or to note some particularly interesting cases. We have made no attempt to provide complete references here; they are in the on-line atlas. For the convenience of the reader, we have collected in Table 5 various basic measurements. These are:

- Spectroscopic class. This is a phenomenological classification based on the appearance of the spectrum in the first few spectra after the emission lines appear. Physically, this is likely an indicator of the optical depth of the envelope. Of the 63 classifiable targets, most (47/63, or 75%) are Fe II type; 15 (24%) are or may be He-N, and one is a possible symbiotic nova. In one case we cannot tell because our first spectrum was obtained nearly 2 years after peak.

We append a “w” in those cases where there is a clear P Cygni absorption in the Balmer lines (and sometimes in Fe II) indicative of an optically-thick wind. Half (32 of the 64 novae) show such P Cyg absorption. We caution that the absence of P Cyg absorption may be caused by the cadence of the observations.

- Photometric class. We examined the V band light curves for the first 500 days and categorized them by eye into one or more of the 7 classes defined by Strope et al. (2010). In many cases we have very little data during the first 3 months, and do not attempt to categorize these. In some cases we had a hard time shoe-horning the lightcurve into one class, and have given multiple classes. For example, N LMC 2005 maintained a fairly flat light curve for about 50 days (class F), then exhibited a cusp (class C). It also formed dust (class D), though the dip is not particularly pronounced. The presence of dust is indicated by the increase in the H and K fluxes as the optical fades.

In many cases a significant brightening in K , suggestive of dust formation, is not accompanied by an optical dip, suggesting an asphericity in the dust.

In some cases there is significant color evolution between the optical and near-IR. We will quantify this later.

- The FWHM of the $H\alpha$ emission line. We measure the first grating 47 spectrum (3.1\AA resolution) that does not show P Cyg wind absorption, and report the day on which that spectrum was obtained. Uncertainties are of order 2%. Note that the FWHM can change significantly with time in the Fe II novae. For the He-N novae we measure the FWHM of the broad base, ignoring the narrow central emission component. In some cases there is a faint but broader component visible early on. The measurement of the FWZI of this component would be more representative of the maximum expansion velocity. We do not tabulate this because of incompleteness, and because of the difficulty defining the continuum level in some cases.

We have not estimated the times for the light to decay by 2 and 3 magnitudes at V (t_2 and t_3 , respectively) in any systematic manner, because it is only in rare cases that we have sufficiently dense photometric sampling early enough to make a good estimate. We discuss these in the notes on individual novae.

We note that the estimates of t_2 and t_3 can be highly uncertain, especially for fast novae. The reported discovery times are often past the peak. The discovery magnitudes are often visual estimates, or unfiltered CCD magnitudes, necessitating a color correction to V . A full analysis of the light curves, incorporating other published literature, AAVSO data (which are much denser near peak), and data from other sources, is beyond the scope of this paper.

4.3.1. N Aql 2005 = V1663 Aql

This is a standard Fe II nova. On day 50 there was prominent $\lambda 4640\text{\AA}$ Bowen blend emission. The auroral [O III] lines were strong by day 85. Our last spectrum, on day 414, is dominated by $H\alpha$, [O III] 4959/5007, [N II] 5755, [Fe VII] 6087, [O I] 6300, and [Ar III] 7136.

4.3.2. N Car 2008 = V679 Car

This Fe II nova never seemed to develop a coronal phase. We have limited photometric coverage.

4.3.3. N Car 2012 = V834 Car

This recent Fe II nova exhibited a strong wind through day 36. Evolution of the light curve has been uneventful. There was some jitter of ± 0.5 mag from a smooth trend from days 12-40. We estimate t_2 and t_3 to be 20 and 38 days, respectively, with uncertainties of order ± 3 days for t_2 and ± 1 day for t_3 .

4.3.4. N Cen 2005 = V1047 Cen

We have no photometry, and only two spectra, of this Fe II nova.

4.3.5. N Cen 2007 = V1065 Cen

This dusty Fe II nova was analyzed by Helton et al. (2010), using SMARTS spectra through day 719. The atlas includes additional photometry, from days 944 through 1850.

4.3.6. *N Cen 2009 = V1213 Cen*

This Fe II nova became a bright super-soft X-ray source. The coronal phase extended from about days 300 to 1000, roughly coinciding with the SSS phase (Schwarz et al. 2011), with strong lines of [Fe X], [Fe XI], and [Fe XIV]. In quiescence the remnant is blended with two other objects of comparable brightness.

4.3.7. *PNV J13410800-5815470 = N Cen 2012*

This recent Fe II nova exhibited wind absorption through day 25. t_2 is about 16 ± 1 days; t_3 occurs about day 34. The 2 mag brightening in K starting about day 35, with a contemporaneous drop in the B and V band brightness, suggests dust formation. The strong emission in the Ca II near-IR triplet on day 11 had disappeared by day 74.

4.3.8. *PNV J14250600-5845360 = N Cen 2012b*

The K band brightness increased by 2 magnitudes between days 18 and 32, suggesting dust formation, but no drop is seen at optical magnitudes. The smooth V light curve yields t_2 and t_3 of 12.3 and 19.8 days, with uncertainties < 1 day. The spectral development is similar to N Cen 2012. The strong emission in the Ca II near-IR triplet on day 16 had disappeared by day 61.

4.3.9. *N Cir 2003 = DE Cir*

This fast nova was discovered by Liller (2003) in the glare of the setting Sun. Spectra obtained on days 11 and 12, at high air mass, show this was a He-N nova. We did not obtain any photometry until after it reappeared from behind the Sun. Since then it has been in quiescence at $V \sim 17$, with a variance of ± 0.4 mag. The strongest line in the quiescent spectrum is He II $\lambda 4686 \text{ \AA}$.

4.3.10. *N Cru 2003 = DZ Cru*

This is another nova that was discovered in the west in the dusk twilight. Despite the discussion about the “peculiar” early spectrum (Bond et al. 2003), our spectra show this was an Fe II nova discovered before maximum, as concluded by Rushton et al. (2008).

4.3.11. *N Dor 1937 = YY Dor*

This is the second recurrent nova discovered in the LMC (Liller 2004). It is a fast ($t_2, t_3=4.0, 10.9$ days, respectively) He-N nova with the broad tripartite Balmer lines seen in many fast recurrent novae. An analysis is in preparation.

4.3.12. *N Eri 2009 = KT Eri*

KT Eri is a fast He-N nova with a bright quiescent counterpart. Hounsell et al. (2010) reported a spectacular pre-maximum light curve from the SMEI instrument. The light curve shows two plateaus (Figure 7), much like those seen in U Sco, prior to dropping to quiescence. Jurdana-Šepić (2012) find a 737 day period in the quiescent source from archival plate material. Hung, Chen & Walter (2011) claim a 56.7 day period during the second plateau. In quiescence, after day 650, there are hints of a period near 55 days, and a possibly 4.2 day spectroscopic period (Walter et al. in preparation). Due to its brightness and RA (there is less competition for time towards the galactic anti-center), we have excellent spectral time coverage. Figure 8 shows the time-evolution of KT Eri in the blue, over 790 days, from 83 low dispersion blue spectra.

KT Eri is located in a sparse field; there is only a single comparison star available in the small IR channel field of view.

4.3.13. *N Lup 2011 = PR Lup*

The light curve of this slow Fe II nova showed a second maximum about day 3.5. There was little appreciable decay during the first 2 months. Wind absorption was evident through day 58. As of day 300 it has not entered the coronal phase.

4.3.14. *N Mus 2008 = QY Mus*

We picked up this fairly late, but a combination of the spectroscopy and photometry span the time that dust formed. It seems to be a standard Fe II nova that bypassed the coronal phase and is now in the nebular phase.

4.3.15. *N Nor 2005 = V382 Nor*

This appears to be a standard Fe II nova.

4.3.16. *N Nor 2007 = V390 Nor*

We have good spectroscopic coverage of this Fe II nova for 4 months, but no photometry. During this time it did not evolve any hot lines.

4.3.17. *RS Oph*

This is the prototypical long period, wind-driven recurrent nova. The emission lines are narrow. We are continuing observations to characterize it well into quiescence.

4.3.18. *N Oph 2003 = V2573 Oph*

Based on two spectra, this appears to be a standard Fe II nova.

4.3.19. *N Oph 2004 = V2574 Oph*

Our photometric coverage consists of two observations, 4 and 8 years after the eruption. Neither was obtained on a photometric night, so the data are not yet photometrically calibrated. We have good spectroscopic coverage showing the transition from an optically thick pseudophotosphere to the permitted line spectrum in this Fe II nova.

4.3.20. *N Oph 2006 = V2575 Oph*

This is a standard Fe II nova.

4.3.21. *N Oph 2006b = V2576 Oph*

Most photometric observations are in *R* only. It is a standard Fe II nova.

4.3.22. *N Oph 2007 = V2615 Oph*

This is a normal Fe II nova. Photometric coverage begins after 1.5 years.

4.3.23. *N Oph 2008 = V2670 Oph*

This is an Fe II nova.

4.3.24. *N Oph 2008b = V2671 Oph*

This Fe II nova faded rapidly, and was undetectable, except at *R*, after 1 year.

4.3.25. *N Oph 2009 = V2672 Oph*

Munari et al. (2011) reported on this very fast nova. t_2 and t_3 passed before our first photometry; Munari et al. (2011) quote values of 2.3 and 4.2 days, respectively. The spectra and spectral evolution are similar to those of U Sco. We followed this nova spectroscopically through day 31.6, and did not see the deceleration reported by Munari et al. (2011). This has the broadest $H\alpha$ line, at $FWZI \sim 11,000$ km/s, of all the novae in the atlas, exceeding that of U Sco by about 20%.

4.3.26. *PNV J17260708-2551454 = N Oph 2012*

This recent slow Fe II nova showed no significant decline in brightness from days 10 through 90. Then dust formed, with a drop in the *B* and *V* brightness by over 5 magnitudes. The lines are narrow: $FWHM(H\alpha) \sim 950$ km/s. There is little spectral evolution through day 90, with persistent P Cygni line profiles.

4.3.27. *PNV J17395600-2447420 = N Oph 2012b*

This is an Fe II nova with an $H\alpha$ FWHM about 3000 km/s. Through the first 45 days the brightness drops monotonically in *B* through *K*.

4.3.28. *N Pup 2004 = V574 Pup*

See §4.2. Our first photometry was on day 30, suggesting $t_3 < 27$ days. Schwarz et al. (2011) quote $t_2 = 13$ days.

4.3.29. *N Pup 2007 = V597 Pup*

This slowly developing, broad-lined nova developed a coronal phase after 3-4 months.

4.3.30. N Pup 2007b = V598 Pup

This X-ray-discovered nova was in its nebular phase when reported by Read et al. (2007). The quiescent counterpart appears fairly bright.

4.3.31. T Pyx

This well-known recurrent novae is, as has been pointed out by many authors, very different from the fast He-N recurrent novae. Its light curve and spectral development mimic those of slow classical novae. The rate of the photometric decay remained unchanged by the turn-on/turn-off of the SSS X-ray emission (Figure 11). The slope of the photometric decay decreased about day 300. The H α line width shown in Table 5 refers to the width of the broad base after the line profile stabilized; it was about half that during the first 40 days post-peak.

Evans et al. (2012) include some of our near-IR photometry in an analysis of the heating of the dust already present in the system.

As T Pyx remains bright, we are continuing our monitoring.

4.3.32. U Sco

This is the prototypical short orbital period recurrent nova. Some spectral analysis is included in Maxwell et al. (2012).

4.3.33. N Sco 2004b = V1187 Sco

This well-observed Fe II nova became a super-soft X-ray source.

4.3.34. N Sco 2005 = V1188 Sco

We have only limited coverage of this Fe II nova.

4.3.35. N Sco 2007a = V1280 Sco

This extraordinarily slow nova has remained bright (V generally between 10 and 11) for nearly 2000 days. Naito et al. (2012) present a lot of data for this nova; our monitoring provides finer temporal coverage, which show absorption events with durations <60 days that may be due to

dust formation in small mass ejection events. The latest spectra, at an age of 5.3 years, still show evidence for wind absorption.

4.3.36. N Sco 2008 = V1309 Sco

This is a very narrow-lined system, and likely a symbiotic nova or a merger (Mason et al. 2010). The spectrum is dominated by narrow Balmer line emission.

4.3.37. N Sco 2010 No. 2 = V1311 Sco

This nova faded rapidly. It is likely a He-N class nova. On day 9 possible [Ne III] λ 3869 is seen, and the λ 4640 Bowen blend is in emission.

4.3.38. N Sco 2011 = V1312 Sco

This Fe II nova developed coronal line emission.

4.3.39. N Sco 2011 No. 2 = V1313 Sco

This nova exhibited very strong He I and H-Paschen line emission. Strong He II λ 4686 emission appeared between days 16 and 19. The Balmer lines have a narrow central core atop a broad base, as in the He-N and recurrent novae, but there is also likely Fe II multiplet 42 emission at λ 5169Å (other multiplet 42 lines are overwhelmed by He I emission lines), and wind absorption at least through day 3. This seems to be a hybrid nova. t_2 lies between 5.8 and 8.5 days, and t_3 between 13 and 18 days, depending on whether the peak was on 2011 Sep 6.37 or 2011 Sep 7.51 (Seach et al. 2011). The continuum is red. This may be a symbiotic nova.

4.3.40. N Sct 2003 = V475 Sct

This was the first nova that we concentrated on. Results appear in Stringfellow & Walter (2006). This fairly narrow-lined Fe II nova may have formed dust; no coronal phase was seen. We have *U*-band photometry for the first 100 days,

4.3.41. *N Sct 2005 = V476 Sct*

We have very limited observations of this Fe II nova.

4.3.42. *N Sct 2005b = V477 Sct*

This is probably an Fe II nova; we have very poor coverage.

4.3.43. *N Sct 2009 = V496 Sct*

This Fe II nova likely formed dust. As it is fairly bright, we have good spectral coverage for nearly 2 years.

4.3.44. *N Sgr 2002c = V4743 Sgr*

This is the first nova we started observing. We picked it up about 200 days after discovery. There is currently no photometry in the atlas.

4.3.45. *N Sgr 2003 = V4745 Sgr*

This was the first nova to explode during the SMARTS era. There are two prominent P Cygni absorption line systems, initially at -780 and -1740 km/s, visible from days 12 through 66; they disappear by day 71. There is currently no photometry in the atlas.

4.3.46. *N Sgr 2004 = V5114 Sgr*

Data for this Fe II nova have been analyzed and published by Ederoclite et al. (2006). Ederoclite et al. (2006) quote t_2 and t_3 values of 11 and 21 days; for a peak $V=8.38$ we find a marginally slower nova, with t_2 and t_3 of 14 and 25 days, respectively. We have U band photometry for the first 180 days.

4.3.47. *N Sgr 2006 = V5117 Sgr*

This is a standard Fe II nova. We estimate t_2 and t_3 are about 16 ± 1 and 42 days, respectively, with uncertainties of perhaps a week in t_3 .

4.3.48. *N Sgr 2007 = V5558 Sgr*

This very slow nova resembles V723 Cas. We started the photometry at about day 100; the nova remained at $7.0 < V < 9$ through day 200, with the exception of one short dip to $V=10$ seen in all 7 bands. Since then there has been an uneventful decay to $V \sim 14$. It is a narrow-lined Fe II nova that exhibits P Cygni absorption through day 208. He II 4686 exceeded $H\gamma$ in strength by day 480, and rivaled $H\beta$ by day 1100. The [Ne V] doublet was visible by day 432, and became the strongest line, aside from $H\alpha$, by day 1150. There is very strong [Fe VII] emission, but little coronal [Fe X].

4.3.49. *N Sgr 2008 = V5579 Sgr*

This standard Fe II nova apparently formed dust, because it was bright in the near-IR ($K=6.6$) and fainter than 23^{rd} mag at *BVRI* on day 68. When we next looked at it, on day 1120, $V \sim 16.1$ mag with $V - K \sim 1.6$.

4.3.50. *N Sgr 2009 No. 3 = V5583 Sgr*

This appears to be a standard Fe II nova. Linear interpolation between our first 2 observations yields t_2 and $t_3 = 6.7$ and 12.6 days, respectively; Schwarz et al. (2011) quotes $t_2 \sim 5$ days.

4.3.51. *N Sgr 2009 No. 4 = V5584 Sgr*

This appears to be a standard Fe II nova.

4.3.52. *N Sgr 2010 No. 2 = V5586 Sgr*

We have only a single red spectrum of this nova. The broad $H\alpha$ emission line, the presence of strong broad He I lines, and the rapid decay are all consistent with a He-N classification. The nova is located about 2.5 arcsec E of a highly extinguished near-IR source, 2MASS J17530316-2812183. This can contaminate the photometry, particularly on nights with less than ideal seeing.

4.3.53. *N Sgr 2011 No. 2 = V5588 Sgr*

This Fe II nova exhibited at least 6 outbursts of up to 2 mag during the first 200 days. The spectrum shows an Fe II nova with very strong and time-variable He II 4686 and [Fe VII] and [Fe X]

emission lines.

4.3.54. PNV J17452791-2305213 = N Sgr 2012

This fast hybrid nova showed Fe II emission on day 3, but by day 8 resembled a He-N nova. By day 65 it was in its coronal phase, with emission from [Fe X], [Fe XI], and [Fe XIV]. The FWHM of H α is about 5700 km. t_2 passed prior to our first photometric observation, and was likely 4.5 ± 1.5 days; t_3 is about 7 days.

4.3.55. N TrA 2008 = NR TrA

This is the only nova in our collection that has shown eclipses. The 5.25 hour period has a broad primary minimum covering half the period (Figure 9) and a likely smaller secondary minimum.

The early spectra are those of an Fe II nova with narrow lines. The cool permitted lines (N II, He I, Fe II) faded out between days 570 and 1220, and were replaced with a composite of a nebular spectrum with a WN-like spectrum. After the nebular lines of [O III], [Ne V], and [Fe VII], the strongest lines are the Balmer series and He II $\lambda 4686$. Other prominent high excitation lines include He II (4200, 5411, 7592, 8236) N III (4515 and the 4640 blend), N IV and/or N V (4606/4608), C IV (5803), O VI (3811, 5292, 6200), and a strong line that may be a blend of N IV (7703), C IV (7708), and O IV (7713). A recent optical spectrum is shown in Figure 10.

Aside from the nebular lines, the system bears a striking resemblance to the V Sge stars (Steiner & Diaz 1998). Steiner & Diaz (1998) argue that the presence of O VI, and the absence of strong hard X-ray emission, implies the presence of a source of super-soft X-rays, with kT between 30 and 50 eV. This in turn suggests steady nuclear burning in the atmosphere of a massive WD, as in the persistent SSS sources like Cal 83 or RX J0513-69. However, models containing other types of compact objects, or even WC stars, remain viable, and Smak et al. (2001) argue that V Sge is a contact binary following common envelope evolution. However, Hachisu & Kato (2003) conclude that V Sge is the product of accretion wind-driven evolution of a massive WD, similar to the persistent SSS sources.

Since NR TrA, as a classical nova, must contain a WD, if further investigation confirms its resemblance to the V Sge stars then we may be able to clarify the nature of those systems.

4.3.56. PNV18110375-2717276 = N Sgr 2012b

This apparently very slow nova was reported in April 2012 (Nakano et al. 2012), and then found to have been bright at least as early as 12 April 2011.

4.3.57. PNV17522579-2126215 = N Sgr 2012c

This nova was reported on 26 June 2012. The single spectrum we have shows a broad H α line, with FWHM 4200 km/s. Both t_2 and t_3 passed prior to our first photometric observations, with $t_3 < 7.5$ days.

4.3.58. N LMC 2005

This is a slow Fe II nova. The light curve was flat for about 2 months, developed a cusp, and then formed dust after about 100 days.

4.3.59. N LMC 2009

This is a recurrence of N LMC 1971b, and becomes the third known recurrent nova seen in the LMC. It developed into a strong super-soft X-ray source. A full analysis is in preparation (Bode et al. 2012).

4.3.60. N LMC 2009b

This Fe II nova formed dust; there is a very deep trough in the optical light curve between about days 80 and 120, following a 4 mag increase in brightness at K .

4.3.61. N LMC 2012

This is a very fast ($t_2=1.1\pm0.5$ days; $t_3=2.1\pm0.5$ days) recent He-N nova.

4.3.62. CSS081007:050559+054715

This peculiar high galactic latitude object showed triple peaked, velocity-variable H α emission. After [Ne V], the strongest emission line is He II $\lambda 4686\text{\AA}$.

4.3.63. XMMU J115113.3-623730

The spectra nearly 2 years after peak shows strong emission in He II, C IV, N IV, and O VI (see Hughes et al. 2010). We confirm the 8.6 hour period (Patterson et al. 2010). The system bears

some resemblance to high excitation systems like V Sge. The nebular [O III] emission, absent on day 604, appeared about day 800 and now dominates the spectrum (day 1281).

5. Discussion

The nature of our interest in novae has evolved over time, as we have gained experience with these systems. What seemed at first to be a largely understood class of objects has become more and more puzzling as the full scope of the population has become evident.

We are exploiting this database to investigate a number of areas, including:

- The origin and evolution of the tripartite Balmer line profiles in the fast He-N novae. Such novae eject very little mass, hence their envelopes are thin, and afford the opportunity to view the innermost environs of the novae at early times. Walter & Battisti (2011) note the similarity of the tripartite Balmer line profiles to those of optically-thin accretion disks, and suggest that we are seeing either a disk that survives the outburst, or one that reconstitutes itself within a few days of the outburst.
- The relation of the spectral and photometric evolution to the super-soft X-ray emission. The X-rays probe the innermost, hottest regions near the surface of the white dwarf. While the envelope is optically thick to soft X-rays, one can probe hotter regions using the Bowen fluorescence mechanism (McClintock et al. 1975; Kallman & McCray 1980) and the optical He II lines. We are examining how these lines vary with the emergent soft X-ray flux.
- Novae in the LMC. These have the advantage over novae in the Milky Way in that they are at a known distance, and suffer fairly small reddening. They are a small but statistically complete sample that can be used for population studies. A catalog of all known novae in the LMC is maintained at MPE⁶. While a much larger sample of novae at a uniform distance and low reddening exists in M31 (e.g., Pietsch et al. 2007, Shafter et al. 2011), those novae are fainter and the field is more crowded. The novae in the LMC can generally be followed for longer and in more detail than can those in M31.

Novae are complex systems that likely lack spherical symmetry, hence examination of the evolution of a large sample will provide insights into the behaviors that may be masked by geometric effects in particular cases. Our investigations focus on the ensemble for this reason, but there are many other types of investigations that these data can help one address.

⁶www.mpe.mpg.de/~m31novae/opt/lmc/index.php

6. Access to the Data

We are making the data freely available to the community at

<http://www.astro.sunysb.edu/fwalter/SMARTS/NovaAtlas/>

with the following caveats:

- There may be faulty data in the atlas. This includes some early low dispersion spectra (grating 13 setup) that are clearly mis-calibrated. We will correct this as time permits.
- There are some spectra that are clearly not of the correct star. We have tried to catch these, but some certainly have escaped notice.
- There are mis-calibrated or poorly calibrated spectra for the reasons alluded to in §2.1.
- Magnitudes of very faint novae, or novae in crowded regions, should be used with caution. At a later time we may employ PSF-fitting photometry.
- Magnitudes are differential, but corrected for zero-point, and may differ systematically from the truth.
- Some data are not posted, simply because we are currently working on those objects.

If you choose to use any of the data in your research, please reference this paper. Any questions about the data may be directed to the lead author.

The compilation of this atlas would not have been possible had it not been for the vision of Charles Bailyn, who formed the SMARTS partnership in 2003 in order to keep the small telescopes at CTIO, and the science enabled by them, open and accessible to the community.

The reason that SMARTS is a success is due in large part to its cadre of service observers, including Claudio Aguilera, Sergio Fernandez, Rodrigo Hernandez, Manual Hernandez, Alberto Miranda, Alberto Pasten, Jacqueline Seron, and Jose Velasquez. They have taken the vast majority of the observations available in the atlas. Their professionalism ensures the uniformly excellent quality of the data. Eduardo Cosgrove and Arturo Gomez have been invaluable in keeping the telescopes and instruments running. We are thankful for the efforts of the 1.3m telescope schedulers at Yale, including M. Buxton, R. Chatterjee, and J. Nelan, to accommodate our many requests for prompt scheduling of new novae.

We thank W. Liller for forwarding reports of his discoveries.

FMW is desperately trying to learn enough to expound confidently about novae, and is grateful to B. Schaefer, G. Schwarz, S. Shore, R. Williams, and other members of the *Swift* Nova working group for enlightening discussions.

We acknowledge support from the Provost, the Vice President for Research, and the Department of Physics & Astronomy of Stony Brook University to purchase time at SMARTS. We acknowledge support from HST GO grants to Stony Brook University to obtain ground-based observations in concert with HST UV spectroscopy. HEB acknowledges support from the STScI Director’s Discretionary Research Fund, which supported STScI’s participation in the SMARTS consortium.

REFERENCES

- Bode, M.F. & Evans, A., *Classical Novae, 2nd edition*, 2008, (Cambridge)
- Bond, H.E. et al. 2003, IAUC, 8185
- Dworetzky, M.M. 1982, MNRAS, 203, 917
- Ederoclite, A. et al. 2006 A&A, 459, 875
- Evans, A. et al. 2012, MNRAS, in press
- Ford, H.C. 1978, ApJ, 219, 595
- Hachisu, I. & Kato, M. 2003, ApJ, 598, 527
- Hamuy, M., Walker, A.R., Suntzeff, N.B., Gigoux, P., Heathcote, S.R. & Phillips, M.M. 1992, PASP, 104, 533
- Hamuy, M., Suntzeff, N.B., Heathcote, S.R., Walker, A.R., Gigoux, P. & Phillips, M.M. 1992, PASP, 106, 566
- Helton, L.A. et al. 2010, AJ, 140, 1347
- Hounsell, R. et al. 2010, ApJ, 724, 480
- Hughes, J.P. et al. 2010, ATel, 2771
- Hung, L.W., Chen, W.P. & Walter, F.M. 2012, ASPC, 451, 271
- Jurdana-Šepić, R., Ribeiro, V.A.R.M., Darnley, M.J., Munari, U. & Bode, M.F. 2012, A&A, 537, A34
- Kallman, T. & McCray, R. 1980, ApJ, 242, 615
- Kraft, R.F. 1963, in “Adv. Astr. Ap.”, ed. V. Kopal, 2, 43.
- Landolt, A.U. 1992, AJ, 104, 340
- Liller, W. 2003, IAUC, 219

- Liller, W. 2004, IAUC, 8422
- Mason, E., Diaz, M., Williams, R.E., Preston, G. & Bensby, T. 2010, A&A, 516, 108
- Maxwell, M.P. et al. 2012, MNRAS, 416, 1465
- McClintock, J.E., Canizares, C.R. & Tarter, C.B. 1975, ApJ, 198, 641
- McLaughlin, D.B. 1960, in “Stellar Atmospheres”, ed. J.L. Greenstein, 585
- Munari U., Ribeiro V.A.R.M., Bode M.F. & Saguner T. 2011, MNRAS, 410, 525
- Naik, S., Bannerjee, D.P.K., Ashok, N.M., & Das, R.K. 2010, MNRAS, 404, 367
- Naito, H. et al. 2012, A&A, 543, 86
- Nakano, S. et al. 2012, CBET, 3140
- Oke, J.B. 1990, AJ, 99, 1621
- Patterson, J. et al. 2010, ATel, 2777
- Payne-Gaposchkin, C. 1957, “The Galactic Novae” (North-Holland, Amsterdam)
- Pietsch, W. et al. 2007 A&A, 465, 375
- Read, A.M., Saxton, R.D. & Esquej, P. 2007, ATel 1282
- Rushton, M.T., Evans A., Eyres S.P.S., Van Loon J.T. & Smalley B. 2008, MNRAS, 386, 289
- Schwarz, G.J. et al. 2011, ApJS, 197, 31
- Seach, J. et al. 2011, IAUC, 9233
- Shafter, A.W., Darnley, M.J., Hornoch, K., Filippenko, A.V., Bode, M.F., Ciardullo, R., Misselt, K.A., Hounsell, R.A., Chornock, R. & Matheson, T. 2011, ApJ, 734, 12
- Shore, S.N., Augusteijn, T., Ederoclite, A. & Uthas, H., A&A, 533, 8
- Silviero, A., Munari, U. & Jones, A.F. 2005, IBVS, 5638
- Smak, J.I., Belczyński, K. & Zola, S. 2001, Acta Astron., 51, 117
- Starrfield, S. 1971, MNRAS, 152, 307
- Steiner, J.E. & Diaz, M.P. 1998, PASP, 110, 276
- Stringfellow, G.S. & Walter, F.M. 2006, Ap&SS, 304, 401
- Strope, R.J., Schaefer, B.E., & Henden, A.A. 2010, AJ, 140, 34

Subasavage, J.P et al. 2010, SPIE, 7737, 77371C

Walter, F.M. & Battisti, A. 2011, BAAS, 217, 338.11

Williams, R.E., Hamuy, M., Phillips, M.M., Heathcote, S.R., Wells, L. & Navarette, M. 1991, ApJ, 376, 721

Williams, R.E. 1992, AJ, 104, 725

Williams, R.E., Philips, M.M., & Hamuy, M. 1994, ApJS, 90, 297

Table 1. Spectrograph Setups

Mode	Resolution (\AA)	Filter	Wavelength Range (\AA)
<u>Standard Modes</u>			
13/I	17.2	clear	3146–9374
26/Ia	4.1	clear	3660–5440
47/IIb	1.6	BG39	4070–4744
47/Ib	3.1	GG495	5650–6970
<u>Other Modes</u>			
9/I	8.6	clear	3500–6950
47/II	1.6	CuSO ₄	3878–4552
58/I	6.5	GG495	6000–9000

Table 2. Observational Details - “Old” Novae

Nova	T ₀ ^a	Photometry			Spectroscopy				
		Nights	Start	End	V	Nights	Start	End	
N Aql 2005	V1663 Aql	3530.7	32	12.0	2264.9	>22	16	48.9	414. 0
N Car 2008	V679 Car	4797.8	39	75.0	1255.8	18.5	51	3.1	606. 7
N Cen 2005	V1047 Cen	3614.5	0	—	—	—	2	4.9	6. 9
N Cen 2007	V1065 Cen	4123.9	9	14.9	1850.9	18.1	52	5.9	715. 9
N Cen 2009	V1213 Cen	4959.7	55	88.8	1122.8	>17	31	118.9	1016. 9
N Cir 2003	DE Cir	2921.5	99	161.2	3173.1	17.2	62	11.0	3074. 2
N Cru 2003	DZ Cru	2871.9	0	—	—	—	6	1.6	21.6
N Eri 2009	KT Eri	5150.1	265	18.5	890.3	15.4	368	12.5	845. 3
N Lup 2011	PR Lup	5784.	40	1.6	310.6	15.0	36	-1.5	299.6
N Mus 2008	QY Mus	4738.5	67	134.2	1317.1	16.3	40	86.3	1224. 3
N Nor 2005	V382 Nor	3442.8	19	307.1	2556.0	17.6	14	11.9	521. 8
N Nor 2007	V390 Nor	4268.2	0	—	—	—	34	4.6	128. 3
N Oph 1898	RS Oph	3779.3	57	15.5	2303.5	11.6	87	23.6	2022. 3
N Oph 2003	V2573 Oph	2018.3	0	—	—	—	2	822.4	823.4
N Oph 2004	V2574 Oph	3110.3	2	1573.4	2901.5	—	50	1.4	851. 4
N Oph 2006	V2575 Oph	3775.9	17	16.0	1135.9	>22	5	27.0	869. 7
N Oph 2006b	V2576 Oph	3832.1	16	9.7	2179.7	19.7(R)	17	32.7	191. 4
N Oph 2007	V2615 Oph	4179.3	6	18.2	1619.3	21.0	13	11.5	149. 3
N Oph 2008	V2670 Oph	4612.5	13	31.3	1445.2	20.8	18	22.3	480. 0
N Oph 2008b	V2671 Oph	4618.1	9	25.7	1389.8	>22	14	16.7	383. 7
N Oph 2009	V2672 Oph	5060.0	74	3.6	1021.7	19.6	17	3.6	31. 6
N Pup 2004	V574 Pup	3330.2	100	9.1	2723.3	17.9	107	1.7	2607. 7
N Pup 2007	V597 Pup	4418.7	7	31.1	1592.9	19.6	49	28.0	393. 0
N Pup 2007b	V598 Pup	4381.5	5	68.3	1639.1	15.5	26	62.2	422. 2
N Pyx 1890	T Pyx	5664.5	98	1.5	399.5	14.3	155	-26.4	367. 5
N Sco 1863	U Sco	5224.5	0	—	—	—	44	1.4	84. 3
N Sco 2004b	V1187 Sco	3221.1	56	5.5	2777.7	21.5	51	9.5	659. 5
N Sco 2005	V1188 Sco	3576.8	0	—	—	—	10	2.9	56. 7
N Sco 2007a	V1280 Sco	4136.4	94	30.5	1968.3	10.4	194	1.5	1939. 4
N Sco 2008	V1309 Sco	4712.0	17	48.5	1343.9	19.1	24	4.6	63. 5
N Sco 2010 No. 2	V1311 Sco	5312.3	24	27.4	741.4	20.7	3	9.5	73. 5
N Sco 2011	V1312 Sco	5713.6	46	2.2	368.1	17.8	28	2.2	362. 2
N Sco 2011 No. 2	V1313 Sco	5810.4	31	6.2	273.4	17.4	36	2.2	267. 4
N Sct 2003	V475 Sct	2880.1	101	2.5	2386.8	19.5	69	4.4	1771. 6
N Sct 2005	V476 Sct	3643.9	3	19.6	2367.9	>24	2	33.6	34. 6
N Sct 2005b	V477 Sct	3654.5	1	24.0	—	14.6	2	23.0	25. 0
N Sct 2009	V496 Sct	5143.9	48	5.6	939.0	14.5	29	1.6	688. 7

Table 2—Continued

Nova	T_0^a	Photometry			Spectroscopy				
		Nights	Start	End	V	Nights	Start	End	
N Sgr 2002c	V4743 Sgr	2537.9	0	—	—	—	80	206.0	1077.6
N Sgr 2003	V4745 Sgr	2755.2	0	—	—	—	70	4.4	880
N Sgr 2004	V5114 Sgr	3080.3	49	2.5	2357.4	20.0	77	3.5	797.5
N Sgr 2006	V5117 Sgr	3783.9	19	8.0	2217.0	21.6	22	21.0	235.7
N Sgr 2007	V5558 Sgr	4291.5	123	18.2	1880.5	13.9	235	55.4	1876.6
N Sgr 2008	V5579 Sgr	4575.3	11	68.5	1506.5	16.6	15	9.4	1195.4
N Sgr 2009 No. 3	V5583 Sgr	5050.0	35	3.7	991.9	16.5	25	4.7	91.5
N Sgr 2009 No. 4	V5584 Sgr	5130.9	24	2.6	954.9	18.6	9	1.6	355.6
N Sgr 2010 No. 2	V5586 Sgr	5310.3	19	29.4	771.5	17.9	1	5.4	—
N Sgr 2011 No. 2	V5588 Sgr	5648.3	72	30.5	437.5	18.0	54	35.5	427.5
N TrA 2008	NR TrA	4558.2	71	85.5	1547.5	16.3	58	5.5	1523.4
CSS081007:030559+054715	HV Cet	4746.5	19	276.4	1213.1	19.0	29	30.2	130.0
XMMU J115113.3-623730		4793.5	49	613.0	1290.1	15.1	74	604.0	1282.0

^aReference Julian date. This is usually the time of discovery or the time of peak observed brightness.

Table 3. Observational Details - Recent Novae

Nova ^a	T_0^b	Photometry			Spectroscopy				
		Nights	Start	End	V	Nights	Start	End	
N Car 2012	V834 Car	5984.0	35	12.6	125.4	15.5	11	9.4	94.5
PNV J13410800-5815470	N Cen 2012	6009.9	26	2.8	99.7	14.7	17	3.9	95.6
PNV J14250600-5845360	N Cen 2012b	6022.3	14	9.4	83.2	17.6	18	4.3	77.3
PNV J17260708-2551454	N Oph 2012	6012.3	25	11.3	97.5	18.1	19	10.6	91.2
PNV J17395600-2447420	N Oph 2012b	6067.0	12	3.8	41.8	15.3	10	3.9	36.5
PNV J17452791-2305213	N Sgr 2012	6038.5	40	8.3	70.3	15.3	25	2.4	67.0
	N Sco 2012	6085.8	0	—	—	—	3	13.9	17.8
PNV J17522579-2126215	N Sgr 2012c	6105.8	0	—	—	—	2	3.8	8.4
PNV J18110375-2717276	N Sgr 2012b	6000	0	—	—	—	2	435.4	437.3

^aNova designations in the second column have not been authorized by the GCVS, and are unofficial.

^bReference Julian date-2450000. This is usually the time of discovery or the time of peak observed brightness.

Table 4. Observational Details - Novae in the LMC

Nova	T ₀ ^a	Photometry			Spectroscopy				
		Nights	Start	End	V	Nights	Start	End	
N Dor 1937	YY Dor	3298.7	167	1.1	2765.8	18.9	36	1.1	112.9
N LMC 2005		3696.9	152	7.1	2278.0	>19.6	105	7.2	670.2
N LMC 2009		4867.6	143	2.0	1198.9	20.1	53	2.0	187.3
N LMC 2009b		4956.5	47	11.0	1018.1	18.7	41	8.0	261.1
N LMC 2012		6012.9	34	1.6	90.0	18.4	18	0.6	45.6

^aReference Julian date. This is usually the time of discovery or the time of peak observed brightness.

Table 5. Nova Characteristics

Nova		Spec Type	FWHM(H α) (\AA)	day	Phot Type ^a
N Aql 2005	V1663 Aql	Fe II	39	49.0	-
N Car 2008	V679 Car	Fe II	44	4.1	-
N Car 2012	V834 Car	Fe IIw	41	76.5	S
N Cen 2005	V1047 Cen	Fe II	28	6.9	-
N Cen 2007	V1065 Cen	Fe IIw	45	13.9	-
N Cen 2009	V1213 Cen	Fe II	39	125.8	-
PNV J13410800-5815470	N Cen 2012	Fe IIw	31	28.9	S,P,D
PNV J14250600-5845360	N Cen 2012b	Fe II	36	12.5	S
N Cir 2003	DE Cir	He-N	133	12.0	-
N Cru 2003	DZ Cru	Fe IIw	28	20.6	-
N Dor 1937	YY Dor	He-N	145	5.1	S
N Eri 2009	KT Eri	He-N	98	23.6	P
N Lup 2011	PR Lup	Fe IIw	31	19.5	F
N Mus 2008	QY Mus	Fe IIw	34	185.9	D?
N Nor 2005	V382 Nor	Fe II	34	56.9	-
N Nor 2007	V390 Nor	Fe IIw	28	13.4	-
N Oph 1898	RS Oph	He-N	22	25.6	P
N Oph 2003	V2573 Oph	Fe IIw	29	822.4	-
N Oph 2004	V2574 Oph	Fe IIw	36	30.3	-
N Oph 2006	V2575 Oph	Fe IIw	29	94.0	-
N Oph 2006b	V2576 Oph	Fe IIw	55	45.7	S
N Oph 2007	V2615 Oph	Fe IIw	^b	-	-
N Oph 2008	V2670 Oph	Fe II	28	26.3	-
N Oph 2008b	V2671 Oph	Fe II	28	20.7	-
N Oph 2009	V2672 Oph	He-N	190	3.6	S
PNV J17260708-2551454	N Oph 2012	Fe IIw	20	36.6	D
PNV J17395600-2447420	N Oph 2012b	Fe II	66	3.9	S
N Pup 2004	V574 Pup	Fe IIw	51	9.6	S
N Pup 2007	V597 Pup	He-N?	79	31.1	-
N Pup 2007b	V598 Pup	Fe II	50	68.3	-
N Pyx 1890	T Pyx	Fe IIw	73	194.8	S
N Sco 1863	U Sco	He-N	148	3.4	-
N Sco 2004b	V1187 Sco	Fe IIw	64	18.6	S
N Sco 2005	V1188 Sco	Fe II	35	43.8	-
N Sco 2007a	V1280 Sco	Fe IIw	23	55.5	-
N Sco 2008	V1309 Sco	Sy?	4	7.6	-

Table 5—Continued

Nova		Spec Type	FWHM(H α) (\AA)	day	Phot Type ^a
N Sco 2010 No. 2	V1311 Sco	He-N?	79	46.5	S
N Sco 2011	V1312 Sco	Fe IIw	39	2.2	O
N Sco 2011 No. 2	V1313 Sco	He-Nw	94	6.1	S
N Sco 2012		Fe II	45	15.8	D
N Sct 2003	V475 Sct	Fe IIw	30	53.4	F
N Sct 2005	V476 Sct	Fe II	26	33.6	-
N Sct 2005b	V477 Sct	Fe II	56	23.0	-
N Sct 2009	V496 Sct	Fe IIw	26	215.0	-
N Sgr 2002c	V4743 Sgr	Fe II	43	221.9	-
N Sgr 2003	V4745 Sgr	Fe IIw	38	102.5	-
N Sgr 2004	V5114 Sgr	Fe IIw	42	28.4	S
N Sgr 2006	V5117 Sgr	Fe IIw	35	49.9	S
N Sgr 2007	V5558 Sgr	Fe IIw	20	141.2	F
N Sgr 2008	V5579 Sgr	Fe IIw	45	1123.5	-
N Sgr 2009 No. 3	V5583 Sgr	Fe II	66	4.7	S
N Sgr 2009 No. 4	V5584 Sgr	Fe IIw	26	11.6	-
N Sgr 2010 No. 2	V5586 Sgr	He-N?	84	5.4	-
N Sgr 2011 No. 2	V5588 Sgr	Fe II	16	44.6	J
PNV J17452791-2305213	N Sgr 2012	He-N	132	10.4	S
PNV J18110375-2717276	N Sgr 2012b	Fe II	8	101.6	-
PNV J17522579-2126215	N Sgr 2012c	He-N	92	4.5	S
N TrA 2008	NR TrA	Fe IIw	19	29.5	-
CSS081007:030559+054715	HV Cet	He-N	^c	-	-
XMMU J115113.3-623730	—	^d	24	604.0	-
N LMC 2005		Fe IIw	20	20.1	F,D,C
N LMC 2009		He-Nw	96	4.0	P
N LMC 2009b		Fe IIw	22	82.4	D
N LMC 2012		He-Nw	171	2.6	S

^aTypes from visual comparison to Strope et al. (2010) Figure 2.

^bNo H α spectrum available.

^cH α line profile is peculiar.

^dFirst spectrum obtained too late to classify nova type.

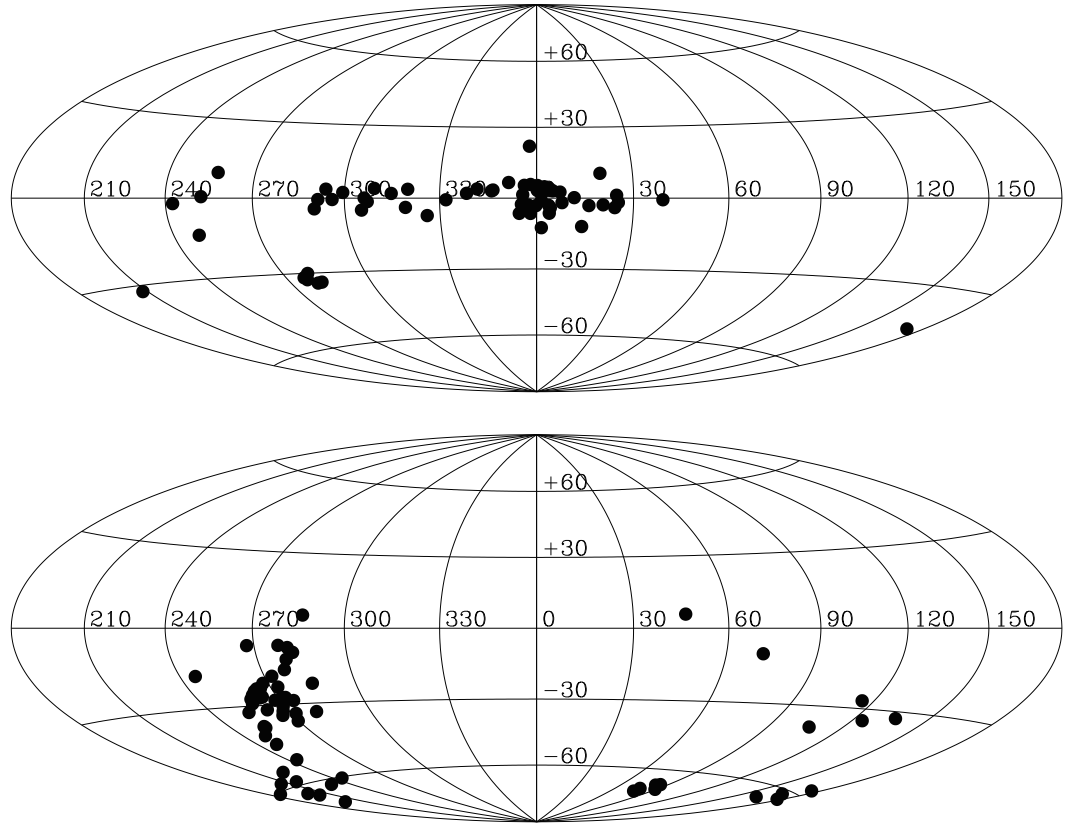
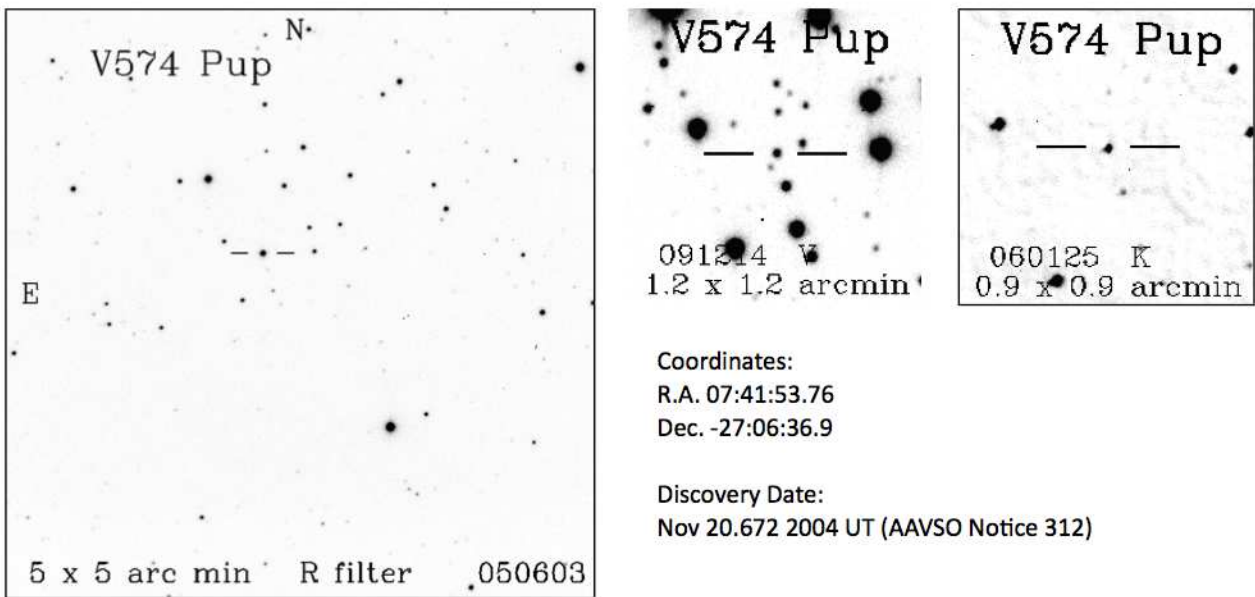


Fig. 1.— The spatial distribution of the novae currently in the atlas. The lower plot shows the distribution in celestial coordinates, centered at RA=0.0; the upper plot shows the distribution in galactic coordinates, centered at $\ell^{II}, B^{II}=0,0$.

[Atlas Home](#)

V574 Pup (Nova Pup 2004)



[Available Spectra](#)

2004 Nov 12 -

[Other](#)

[Photometry](#)

2004 Dec 23 through
(JD 2453362.727 JD -)

[References](#)

Fig. 2.— The main atlas page for V574 Pup. The large finding chart shows the nova at an age of about 8 months. The smaller charts, each ~ 1 arcmin wide, show the nova in *V* and *K* after it has faded substantially from peak.

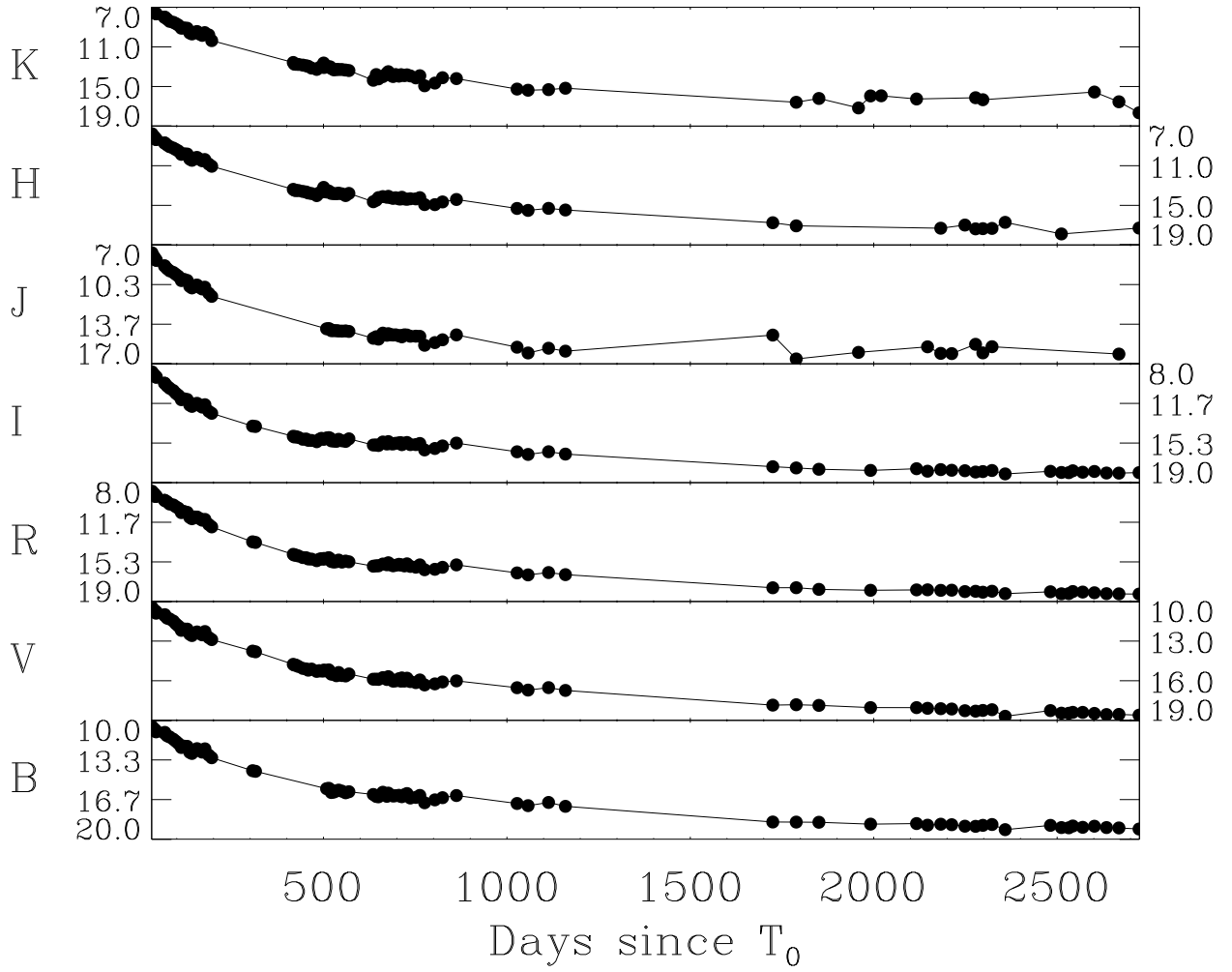


Fig. 3.— SMARTS OIR light curve of V574 Pup from the ANDICAM dual channel imager. We observed on 100 days, starting on day 33 and running through day 2723. The near-IR source is near the detection limit after day 1500; only points with formal uncertainties < 0.5 mag are plotted. Error bars are smaller than the size of the points.

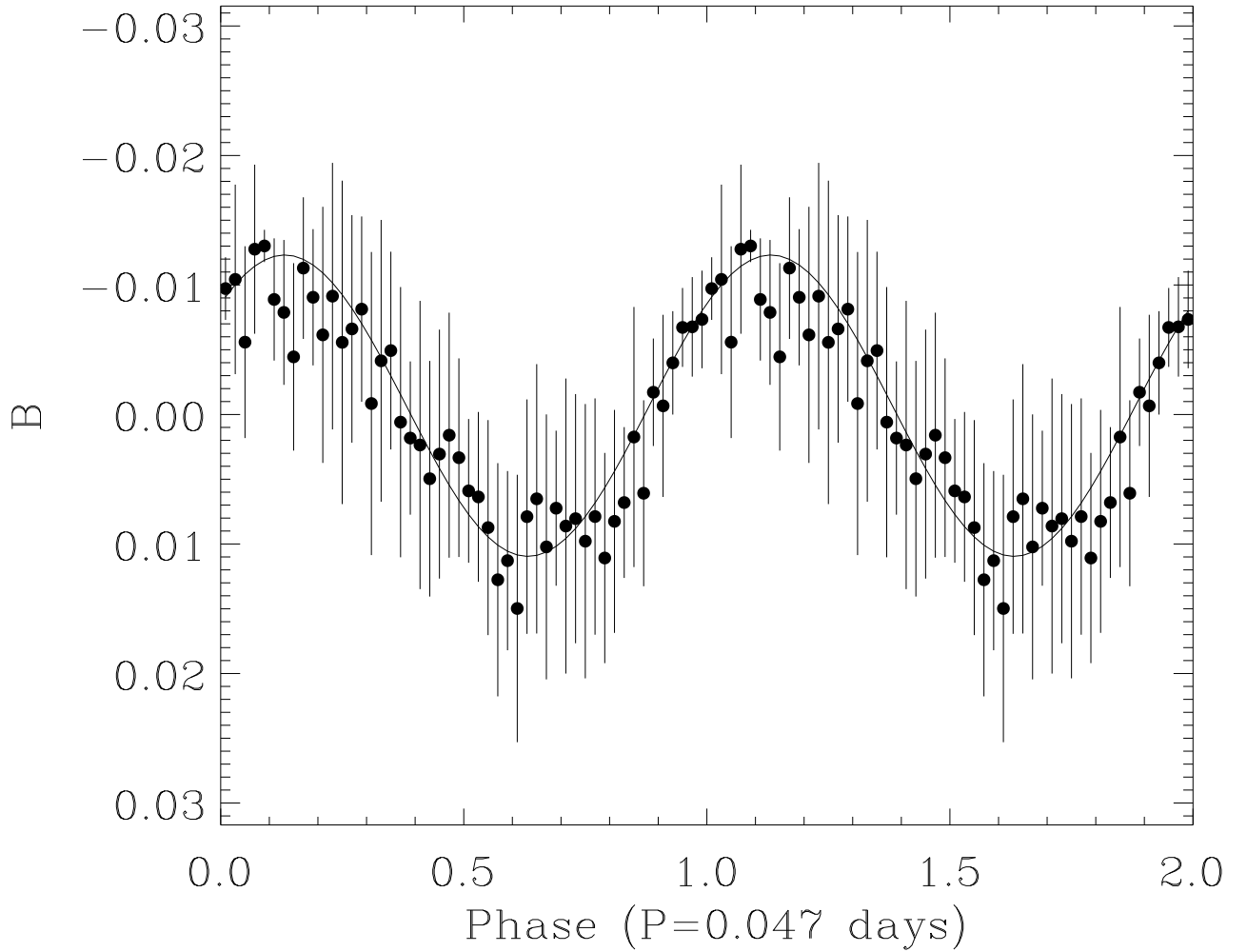


Fig. 4.— 366 B band observations of V574 Pup made on days 87, 195, and 196 using the Apogee 0.5k CCD on the SMARTS 1.0m telescope. The data are folded on the best-fit period; two periods are shown. Phasing is arbitrary. The 0.0472 day period is determined by the shortest string method (Dworetzky 1983); for the plot the data are binned. Error bars represent the dispersion in each 0.02-cycle phase bin.

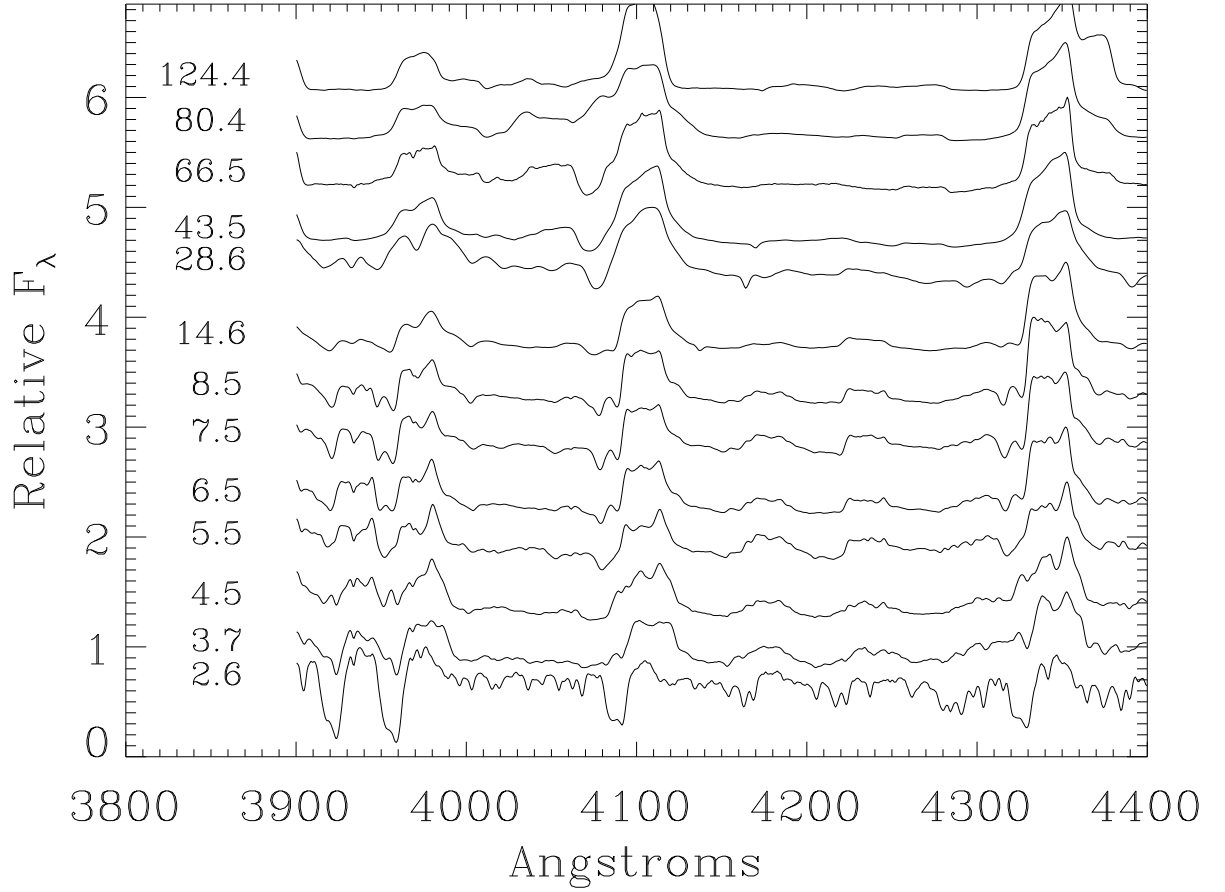


Fig. 5.— The early spectral evolution of V574 Pup in the blue. Spectra are normalized to the peak brightness, and are offset by 0.5 units. The epoch in days is on the left of the spectra. Resolution is 4.4\AA on days 66 and 80, and 1.6\AA otherwise. The strong P Cygni absorption in Ca II K&H and the Balmer lines fades rapidly. The two distinct absorption features seen in the absorption blueward of H δ and H γ seem to accelerate outward at different rates.

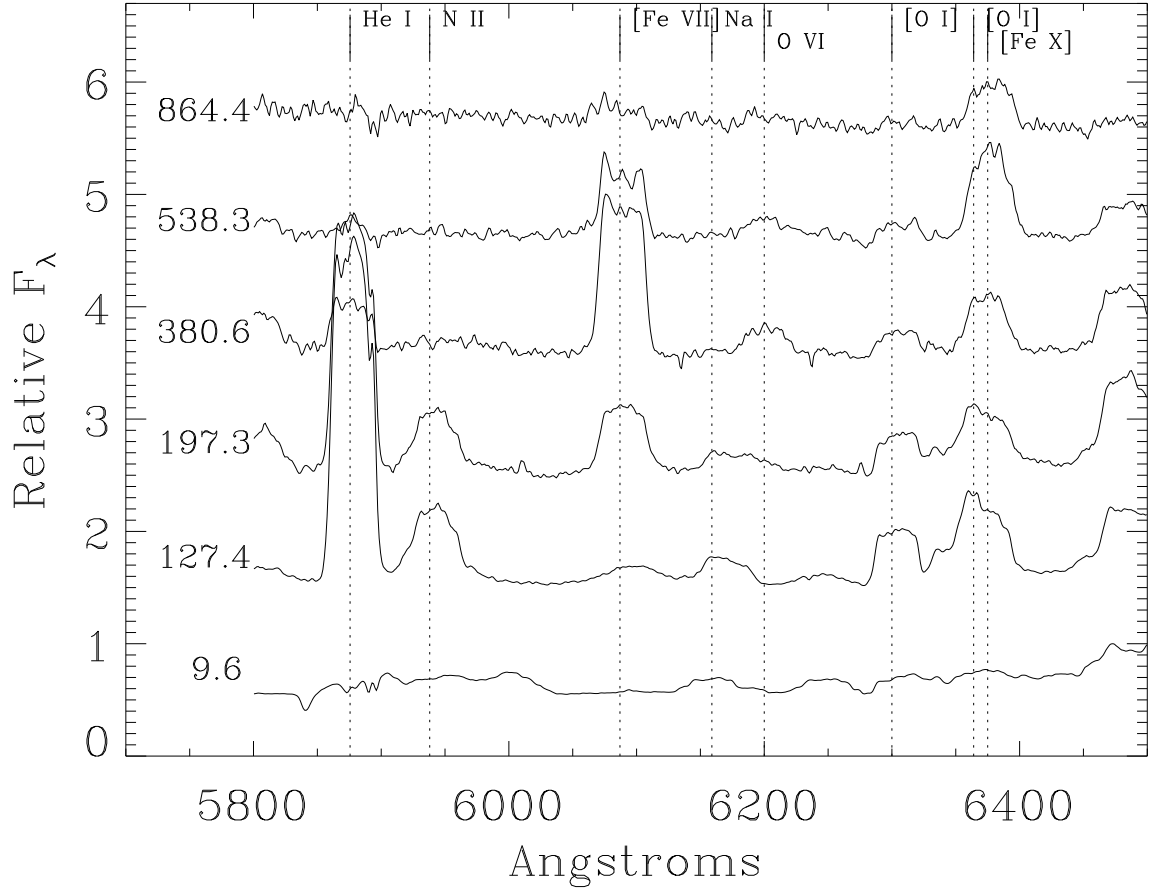


Fig. 6.— The temperature evolution of V574 Pup from days 10 through 864. Spectra are normalized to the peak brightness, and are offset by 0.5 units. The epoch in days is on the left of the spectra. Resolution is 3.1\AA . The first spectrum (day 9.6) is dominated by continuum. Wind absorption from He I 5876 is seen, as are the interstellar sodium absorption lines. By day 127 low excitation lines of He I, N II, and [O I] become important. The nebular [Fe VII] and [Fe X] lines strengthen later, peaking relative to the continuum after about 1 and 2 years respectively. We show 6 of the 35 red spectra of V574 Pup, so a much finer time analysis is possible.

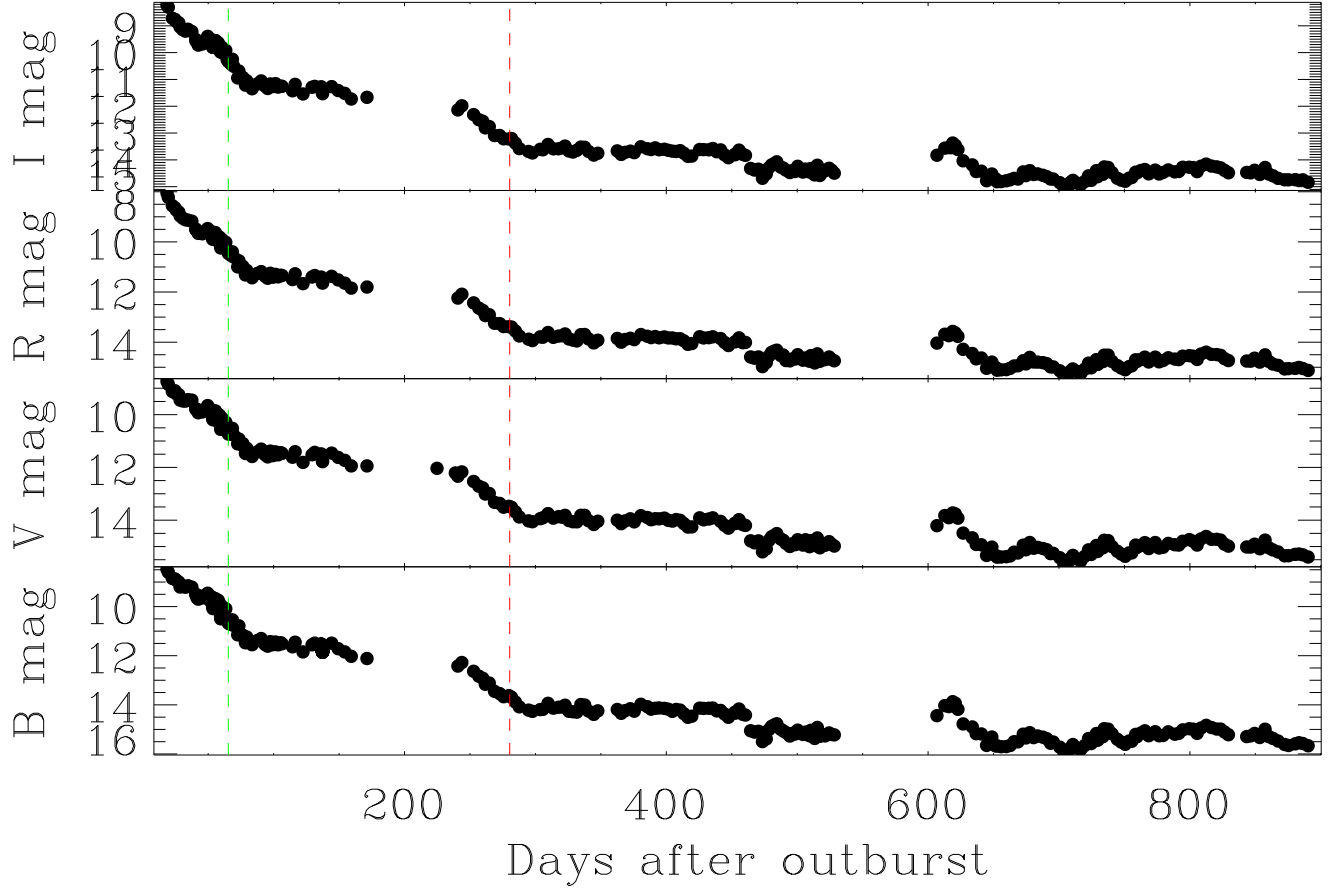


Fig. 7.— The *BVRI* light curves of KT Eri from day 18 through day 890. The two wide gaps in the data are where KT Eri is too close to the Sun to be observed. The initial decay terminates about day 80, 2 weeks after the turn-on of the supersoft X-ray source. Enhanced photometric scatter precedes the X-ray turn-on by about 20 days. The first plateau runs from about days 80 through 210, followed by a 2 magnitude fading over the next 3 months. The second plateau seems to terminate with an abrupt 1 magnitude drop about day 460 to the level seen in archival plates. Since then it has remained near $V=15$, with an RMS scatter of 0.4 mag. The vertical dashed lines indicate the times of the turn-on and turn-off of the bright super-soft X-ray source.

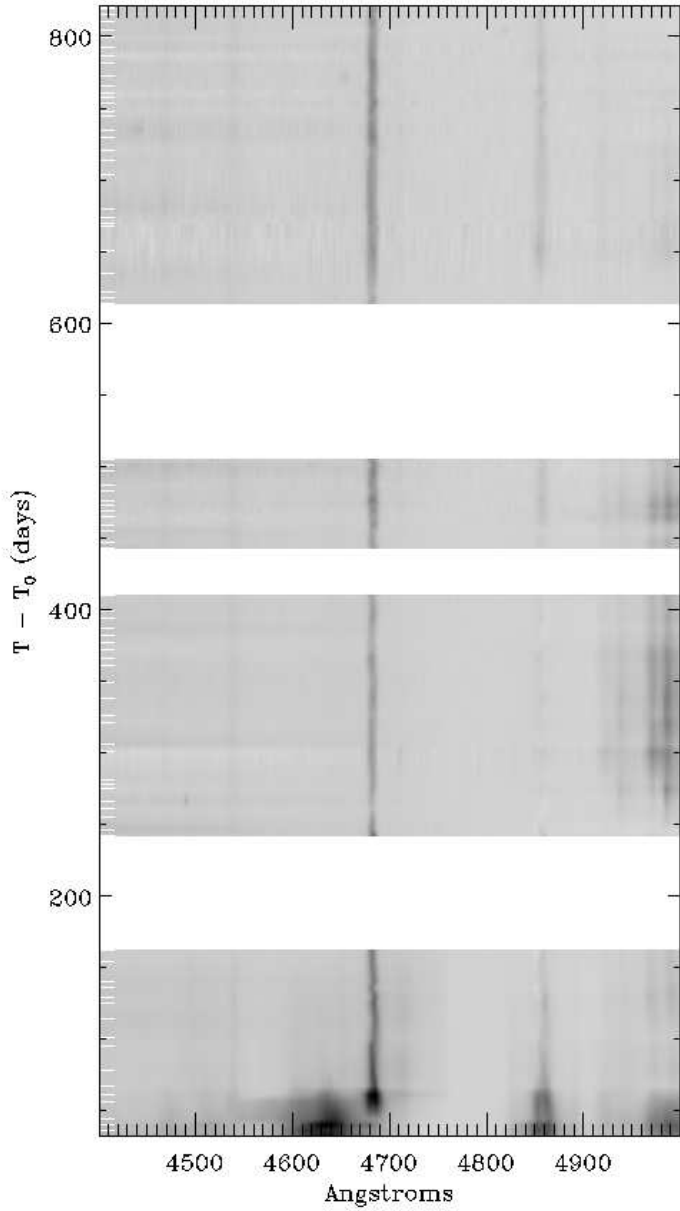


Fig. 8.— The trailed spectrum of KT Eri from day 32 through day 822, constructed from 83 spectra (mode 26/Ia). The times the spectra were obtained are indicated by the white ticks on the left axis. Data are linearly interpolated between spectra for gaps less than 30 days. The data are scaled to the 4750 – 4820Å continuum; the intensity scaling is linear. During the first two months the 4640Å Bowen blend faded, He II λ 4686 turned on, and the $H\beta$ line narrowed considerably, as did the [O III] $\lambda\lambda$ 4959,5007Å lines. There is considerable intensity evolution in the [O III] lines. The late-time spectrum is dominated by He II.

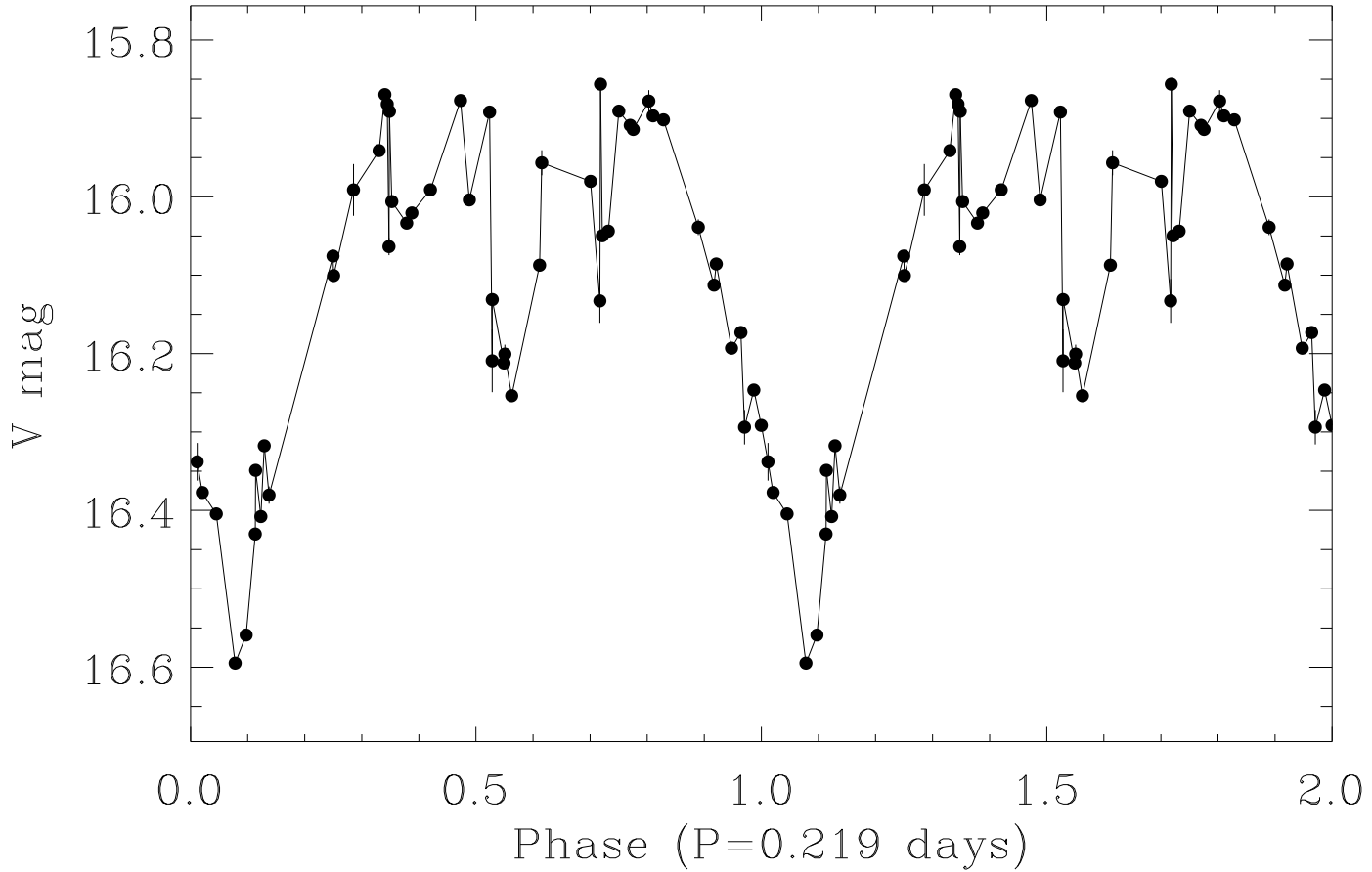


Fig. 9.— The V band light curve of NR TrA from days 1398 through 1534 after peak, folded on the 5.25 hour period. Two cycles are plotted. The broad dip covers nearly 0.5 cycles, is about 0.7 mag deep, and is triangular in shape. There may be a secondary dip in anti-phase, but there also appears to be variability at the 0.1 mag level at all phases. The BRI light curves are similar. 51 observations make up this light curve.

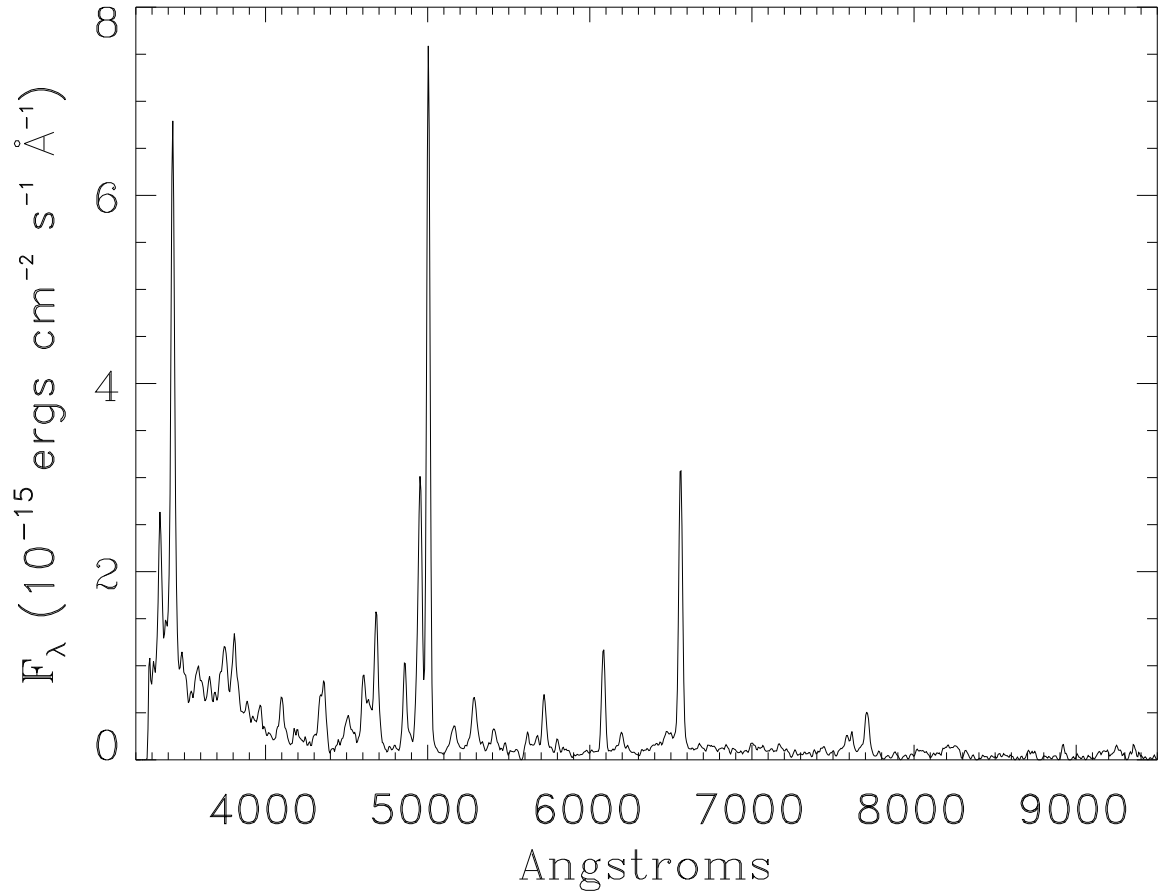


Fig. 10.— The full optical spectra (13/I mode) of NR TrA on 15 March 2012 (day 1444). The nova is classified as nebular (Williams 1991) because the strongest non-Balmer line is [O III] λ 5007. Aside from the nebular lines, strong permitted lines of He II, N III, N IV or N V, and O VI are visible.

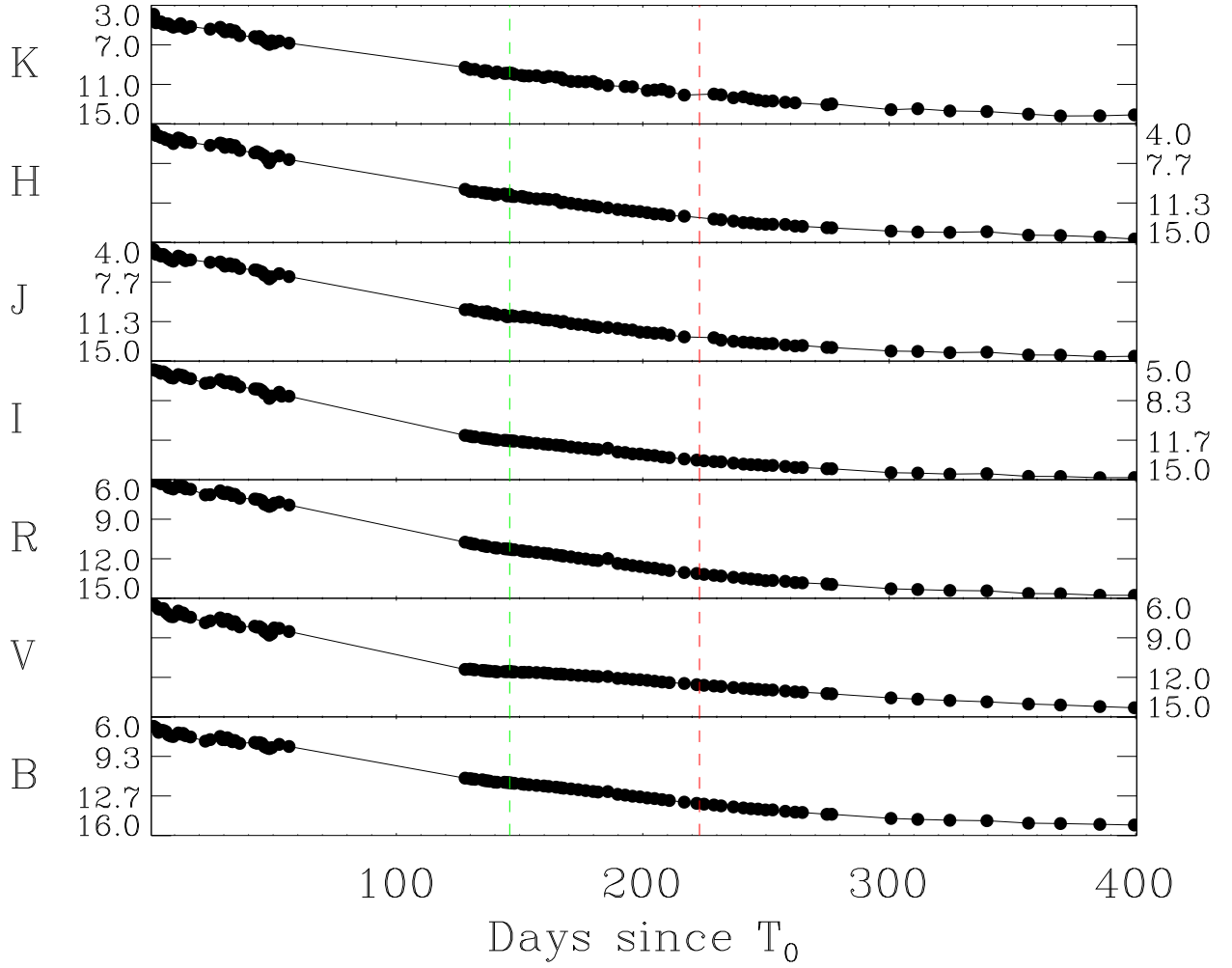


Fig. 11.— The post-peak OIR light curve of T Pyx. The dashed lines represent the approximate times of the turn-on and turn-off of the super-soft X-ray emission. Note that there is neither a plateau in the light curve nor any change in the slope of the decay near these times. The rate of decay did slow between days 250 and 300.